Stochastic model of liquid fuel spraying at high pressures and high Reynolds numbers

ASKAROVA A.S., BOLEGENOVA S.A., MAXIMOV V.YU., BEKETAYEVA M.T.
Physics and Technology Faculty
Al-Farabi Kazakh national university
Almaty, Al-Farabi av., 71
REPUBLIC OF KAZAKHSTAN

Abstract: - The paper describes the main features of the combustion of liquid fuel injections, developed a stochastic model for the atomization of liquid fuels injected into the combustion chamber at high pressures and high Reynolds numbers. A mathematical model for the combustion of liquid injections at high pressures and high Reynolds numbers is presented, which includes: the equations of continuity, motion, internal energy, the K-ε model of turbulence, a system of equations describing the processes of evaporation, mixing, rupture and coalescence of liquid fuel droplets. A stochastic model of atomization of liquid fuels injected into a combustion chamber at high pressures and high Reynolds numbers has been developed. On the basis of the proposed model, computational experiments were carried out to study the combustion of liquid fuel depending on the injected mass in the combustion chamber under given initial conditions in full. When studying the effect of the mass of liquid fuel on the processes of ignition and combustion at high pressures and high Reynolds numbers, the mass values for octane 6 mg and for dodecane 7 mg were taken as the most optimal. A further increase in the injection mass, both for octane and dodecane at optimal pressures, worsens the combustion process. The results obtained are of fundamental and practical importance and can be used to develop the theory of combustion of gaseous and liquid fuels.

Key-Words: - Atomization, high pressure, ignition, injection, numerical simulation, simulation, Reynolds number, turbulent flows, two-phase media, 3D visualization

Received: July 21, 2021. Revised: March 11, 2022. Accepted: April 13, 2022. Published: May 5, 2022.

1 Introduction

Currently, the main source of generated energy (about 80%) is the energy of various types of fuels. Combustion will continue to be the main source of energy for many years to come, even as the use of nuclear energy in industrialized countries expands, and methods of using solar, wind and tidal energy are intensively developed. The problem of the formation of harmful substances and the limited resources of fuel leads to the need to organize more economical methods of its combustion [1-4].

The combustion of liquid fuels is distinguished by a number of specific features due to the occurrence of chemical reactions under conditions of dynamic and thermal interaction of reagents, intensive mass transfer during phase transformations, as well as the dependence of the process parameters on both the thermodynamic state of the system and its structural characteristics.

Since the study of combustion is impossible without its detailed study, the problem of fundamental research into the regularities of heat and mass transfer processes during the combustion of various types of fuels comes to the fore.

Numerical study of the combustion of liquid fuels is a complex task of thermal physics, since it requires taking into account a large number of complex interrelated processes and phenomena. Therefore, the computational experiment is becoming an increasingly important element in the study of combustion processes and the design of various devices that use the combustion process [5-8].

2 The main features of the combustion of liquid fuel

2.1 Mathematical model for the formation of combustion of liquid injections at high pressures and high Reynolds numbers

Here, the main features of the combustion of liquid fuel injections are described, a mathematical model

for the formation of combustion of liquid injections at high pressures and high Reynolds numbers is presented: a system of equations describing the combustion process of atomized liquid fuels [9-12]. The initial and boundary conditions of the problem under study on the combustion of liquid fuels in a combustion chamber are given. A stochastic model of atomization of liquid fuels injected into a combustion chamber at high pressures and high Reynolds numbers has been developed.

The continuity equation for the *m*-th component is written as follows:

$$\frac{\partial \rho_m}{\partial t} + \vec{\nabla}(\rho_m \vec{u}) = \vec{\nabla}\left[\rho D \vec{\nabla}\left(\frac{\rho_m}{\rho}\right)\right] + \dot{\rho}_m^c + \dot{\rho}^s \delta_{m1}, \quad (1)$$

where ρ_m – is the mass density of the component *m*,

ρ - total mass density,

u – fluid velocity.

After summing Eq (l) over all phases, the continuity equation for the liquid is obtained:

$$\frac{\partial \rho}{\partial t} + \vec{\nabla}(\rho \vec{u}) = \dot{\rho}^s \quad (2)$$

The momentum transfer equation for the liquid phas

$$\frac{\partial(\rho \vec{u})}{\partial} + \vec{\nabla}(\rho \vec{u} \vec{u}) = -\vec{\nabla} p + A_0 \vec{\nabla}(2/3 \rho k) + \quad (3)$$

$$+ \vec{\nabla} \vec{\sigma} + \rho \vec{g},$$

p – fluid pressure.

The value of A_0 is equal to zero for laminar flows and unity in the case of turbulent flow.

The viscous stress tensor has the form:

$$\sigma = \mu\left[\vec{\nabla}\vec{u} + (\vec{\nabla}\vec{u})^T\right] + \lambda \vec{\nabla}\vec{u} I. \quad (4)$$

Inter v equation:

$$\frac{\partial(\rho \vec{I})}{\partial} + \vec{\nabla}(\rho \vec{u} \vec{I}) = -p \vec{\nabla}(\vec{u} - \vec{u}_0) \vec{I} + \quad (5)$$

$$- \vec{\nabla} \vec{J} + A_0 \rho \vec{g} + \dot{Q}^c$$

$\dot{Q}^c$ – source term due to heat release as a result of a chemical reaction, $\dot{Q}^s$ – the heat that the injected fuel brings.

The equations *k* - ε of the model for the turbulent kinetic energy *k* and its dissipation rate ε have the form:

$$\frac{\partial \rho k}{\partial t} + \vec{\nabla}(\rho \vec{u}) = \frac{2}{3} \vec{\nabla} \vec{u} + \quad (6)$$

$$+ \sigma \cdot \nabla \vec{u} - \left[\left(\frac{\mu}{\mathrm{Pr}_k}\right) \vec{\nabla} k\right] - \rho \varepsilon + r$$

$$\frac{\partial \rho \varepsilon}{\partial t} + \vec{\nabla}(\rho \vec{u}) = \frac{2}{3} c_{\varepsilon 1} - c_{\varepsilon 2} r + \vec{\nabla} \vec{u} +$$

$$+ \vec{\nabla}\left[\left(\frac{\mu}{\mathrm{Pr}_\varepsilon}\right) \vec{\nabla} \varepsilon\right] + \quad (7)$$

$$+ \frac{\varepsilon}{k}\left[c_{\varepsilon 1} \vec{c} \vec{u} - c_{\varepsilon 2} r + c_s \dot{V}\right]$$

The equation of state for a mixture of gases can be written as:

$$p = R_0 T \sum_m (\rho_m / W_m) \quad (8)$$

Specific internal energy:

$$I(T) = \sum_m (\rho_m / \rho) I_m(T) \quad (9)$$

Specific heat capacity at constant pressure has the form:

$$c_p(T) = \sum_m (\rho_m / \rho) c_{pm}(T) \quad (10)$$

Enthalpy:

$$h_m(T) = I_m(T) + R_0 T / W_m, \quad (11)$$

The change in droplet temperature is determined by the energy balance equation:

$$\rho_d \frac{4}{3} \pi r^3 c_l \dot{T}_d - \rho_d 4\pi r^2 R L(T_d) = 4\pi r^2 Q_d, \quad (12)$$

where c_l – the specific heat of the liquid, $L(T_d)$ is the specific heat of vaporization, and Q_d is the thermal conductivity at the droplet surface in a unit volume.

2.2 Stochastic fuel spray model

The task of modeling liquid fuel atomization for each fragment from the injector at high pressures in the combustion chamber, when the Weber and Reynolds numbers are high, is very difficult. To represent the features of this problem, it is necessary to consider the physical parameters of the decay. To do this, consider the main assumptions in our model.

1) At each moment of time, the liquid clot has its own specific geometric configuration. Each geometric configuration is defined by the spatial trajectory of a stochastic particle (FC).

2) At various times, these configurations are represented by an ensemble of independent implementations. Stochastic particles are sprayed through the injector one after another, in this case each particle has its own path, the duration of which will be determined below. We consider that the distribution *f(x, t, r)* is defined so that $f(x,t,r)d^3r$ is the probability of finding the radial position of the surface r, in the direction of the *x* axis, at time *t* in the volume d^3r. Then this distribution takes the following form:

$$f(x,\ t;\ r)=\langle\delta(r(x,t)-r_{FC})\rangle \quad (13)$$

Where r_{FC} – radial position of a stochastic particle.
The spray near the liquid center of the jet or the region of drops has an insignificant volume, but a significant mass compared to the gas in the combustion chamber. Thus, the droplet clusters that will be located near the injector can be determined by the distribution *f(x, t, r)*.
3) Suppose that the radial position of a given stochastic particle $r_{FC,x}$ to different positions along the axis changes step by step, forming a process in which the value $r_{FC,x+\Delta x}$ is obtained by multiplying by an independent random variable. Thus, it has the following form:

$$r_{FC,x+\Delta x}=r_{FC,x}e^{\ln a} \quad (14)$$

Here the random factor $a(0\le\alpha\le1)$ determined by the probability density distribution $q(\alpha)$ at $\int_0^1 q(\alpha)d\alpha=1$. This coefficient determines the fragmentation by scale symmetry $(r\to\alpha r)$ and depends on the probability density distribution $q(\alpha)$, which is basically unknown. However, such fragmentation with a constant frequency T^{-1}, balance equation, particle size distribution over time can be neglected, with increasing spray time, the Fokker-Planck equation is used [9-11]:

$$\frac{\partial f(r,t)}{\partial t}=-\frac{\langle\ln a\rangle}{T}\frac{\partial}{\partial r}rf+\frac{\langle\ln^2\alpha\rangle}{2T}\frac{\partial}{\partial r}r\frac{\partial}{\partial r}rf \quad (15)$$

$f(r,\ t)$ - normal distribution function, $\int_0^\infty f(r)dr=1$ and only the first two logarithmic moments α can change $f(r,\ t)$ and in the same way:

$$\frac{\langle\ln\alpha\rangle}{\langle\ln^2\alpha\rangle}=\frac{\langle\ln r\rangle}{\langle(\ln r-\langle\ln r\rangle)^2\rangle} \quad (16)$$

The stochastic equation for the radial position of a stochastic particle takes the form:

$$r_{FC,x+\Delta x}=r_{FC,x}+\left[\frac{\langle\ln\alpha\rangle}{T}+\frac{\langle\ln^2\alpha\rangle}{2T}\right]r_{FC,x}dt+ +\sqrt{\frac{\langle\ln^2\alpha\rangle}{2T}}r_{FC,x}dW(t) \quad (17)$$

where $r_{FC,x=0}=R_{inj}^{eff}(t)$ is determined using the effective radius of the injector and $dW(t)$ - stochastic Winnner process with $\langle dW(t)\rangle=0$, $[dW(t)]^2=2dt$ [12].
4) Downward in the direction of the *x*-axis, each stochastic particle moves with an axial velocity equal to the effective velocity $u=U_{inj}^{eff}(t)$ at the inlet of the liquid jet. The effective injector radius and effective injection velocity are calculated using the jet narrowing factor C_C [13], which is based on the cavitation number CN:

$$CN:C_C=\left\{0.62\sqrt{1+\frac{1}{CN}},\ 1;\ CN\ge3\right\} \quad (18)$$

There: $U_{inj}^{eff}(t)=\frac{U_{inj}^{\exp}(t)}{C_C}$, $R_{inj}^{eff}(t)=\sqrt{C_C}R_{inj}^{geom}$, where $U_{inj}^{\exp}(t)$ - given injection speed.
5) The three parameters $\langle\ln\alpha\rangle$, $\langle\ln^2\alpha\rangle$ and T must be determined from (9) according to the decay mechanism. In the stochastic simulation of secondary spray in [14], the solution looked like:

$$\frac{\langle\ln^2\alpha\rangle}{\langle\ln\alpha\rangle}=\ln\left(\frac{r_{cr}}{l_0}\right) \quad (19)$$

l_0 - is the size of the "mother" drop formed by fragmentation along scalar symmetry and r_{cr} - the typical droplet size obtained. Currently, it is proposed that the interaction between the accelerated liquid jet and the gas gives an increase in the Rayleigh-Taylor instability and then drops are formed from the free surface kink. In [15], the most unstable wavelength λ_{RT} of the Rayleigh-Taylor instability was derived, which has the form:

$$\langle\ln\alpha\rangle=\ln\left(\frac{r_{crit}}{\lambda_{RT}}\right) \quad (20)$$

$$\langle\ln^2\alpha\rangle=const\cdot\langle\ln\alpha\rangle=const\cdot\langle\ln\alpha\rangle\cdot\ln\left(\frac{r_{crit}}{\lambda_{RT}}\right) \quad (21)$$

Where constant is chosen equal to 0.1..
The typical size r_{cr} is included in the Weber number equation in the form:

$$We_{cr}=\rho_{gas}\left\langle U_{inj}^{eff}\right\rangle^2 r_{cr}/\sigma=1 \quad (22)$$

The lifetime of each stochastic particle is expressed as:

$$T(t)=\frac{1}{V_{bup}}$$
$$\nu_{bup}(t)=\sqrt{\frac{\rho_{gas}}{\rho_{fuel}}}\frac{U_{inj}^{eff}(t)}{R_{inj}^{eff}(t)} \quad (23)$$

If the value of the Weber number is greater than the critical value, the mathematical model of the secondary spray is activated.
We propose a new modification of this condition. When the fuel injection rate decreases:
$\frac{dU_{inj}^{eff}}{dt} < 0$, the mass of liquid fuel injected earlier has a greater velocity than the mass of fuel injected at the next moment. Thus, we present a new expression for the Weber number, which is compared with the critical:

$$We = \max\left[\rho f_{uel}\left(\delta_t U_{inj}^{eff}\right)^2 \frac{r}{\sigma}\right] \rho_g \left|u_g - u_p\right|^2 \frac{r}{\sigma} \quad (24)$$

$\delta_t U_{inj}^{eff}$ - incremental fuel injection rate over time.
The relaxation equation for the droplet radius r takes the following form:

$$\frac{dr}{dt} = \frac{r - r_*(\varepsilon)}{r(\varepsilon)} \quad (25)$$

Radius $r_*(\varepsilon)$ can be determined after turbulent expansion of droplets:

$$r_* = \left(\frac{\nu\sigma}{\varepsilon\rho_1}\right)^{1/3} \quad (26)$$

Parameter $r(\varepsilon)$ can be determined using dimensional analysis. Turbulent expansion of a droplet is affected by three main physical quantities: viscous dissipation in a turbulent gas flow ε, liquid density ρ_1, and surface tension tensor σ. The quantity is dimensionless and has the form:

$$\tau(\varepsilon) = \left(\frac{\sigma^2}{\varepsilon^3 \rho_1^2}\right)^{1/5} \quad (27)$$

We define the intermittency of turbulence using the log-normal distribution of the Obukov viscous dissipation: $x = \frac{\varepsilon}{\langle\varepsilon\rangle}$, where $\langle\varepsilon\rangle$ - viscous dissipation of the standard κ-ε turbulence model:

$$P(x)dx = \frac{1}{\sqrt{2\pi m_2}} \frac{dx}{x} \exp\left(-\frac{\left(\ln x - m_1\right)^2}{2m_2}\right) \quad (28)$$

There $m_1 = \langle \ln x \rangle$ and $m_2 = \left\langle \left(\ln x - m_1\right)^2 \right\rangle$, at $m_2 = -2m_1 = 0.4 \ln\left(\mathrm{Re}^{\frac{2}{4}}\right)$

For a given drop after time, we choose for it the value of ε from the lognormal distribution and obtain a new radius value.

3 Problem formulation and results of 3D visualization

3.1 Problem under study

In this work, two types of liquid fuels were used: octane (C_8H_{18}) and dodecane ($C_{12}H_{26}$). The chemical reactions for these two fuels are shown below:

$2C_8H_{18} + 50O_2 = 16CO_2 + 18H_2O$

$2C_{12}H_{26} + 37O_2 = 24CO_2 + 26H_2O$

Based on the created stochastic model of atomization of liquid fuels injected into the combustion chamber at high pressures and high Reynolds numbers, under given initial and boundary conditions of the problem under study, the combustion of liquid fuels is considered in a model combustion chamber with a nozzle located in the center of the lower part of the chamber, through which the main part of the liquid fuel consumption is supplied to the oxidizer flow (heated air). The combustion process of liquid fuels is considered in a model combustion chamber with a nozzle located in the center of the lower part of the chamber, through which the main part of the liquid fuel flow is supplied to the oxidizer flow (heated air). The chamber has a cylinder structure 15 cm high and 2 cm in radius. The initial temperature in the combustion chamber is 800 K. The number of control cells is 600. The temperature of the combustion chamber walls is 353 K. The area of the injector nozzle is 2×10^{-4} cm^2 [16].

3.2 Results of computer experiments

The results of computer experiments on the effect of the mass of injected fuel (octane and dodecane) into the combustion chamber on the combustion process, which were carried out by us at optimal pressure values in the combustion chamber.
For octane, the optimal pressure is 100 bar and 80 bar for dodecane, while the mass of injected fuel varied from 4 to 20 mg.
Further, it will be expedient to present graphs only for the optimal mass values for octane 6 mg and dodecane 7 mg.
At high pressure, visualization of the distribution of droplets of two fuels by size at different points in time (Fig. 1-2) and temperature profiles in the space of the combustion chamber at the moment of ignition of liquid fuel (Fig. 3) are plotted.
Analyzing the data obtained, we can say that high pressure leads to a decrease in the spray area, which is quite natural, since the injected liquid experiences greater resistance. At a pressure of 100 bar, the

maximum height of the octane spray area is 0.24 cm, and the width is 0.02 cm, and its droplet sizes range from 6 to 40 μm at the initial spray moment $t=10^{-4}$ (Fig. 1a). A further increase in the octane injection time ($t=3.9\cdot10^{-4}$s) leads to an increase in the area of droplet propagation up to 0.45 cm in height and up to 0.04 cm in width (Fig. 1b). At the final moment of spraying time ($t=1.1\cdot10^{-3}$s), the area of distribution of droplets decreases, which indicates intensive evaporation of liquid fuel (Fig. 1c).

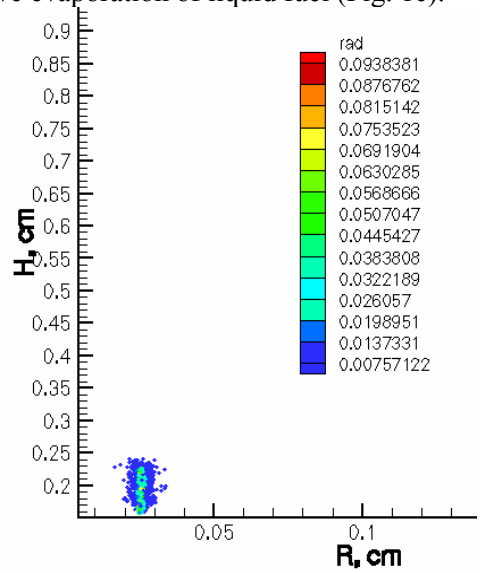

a)

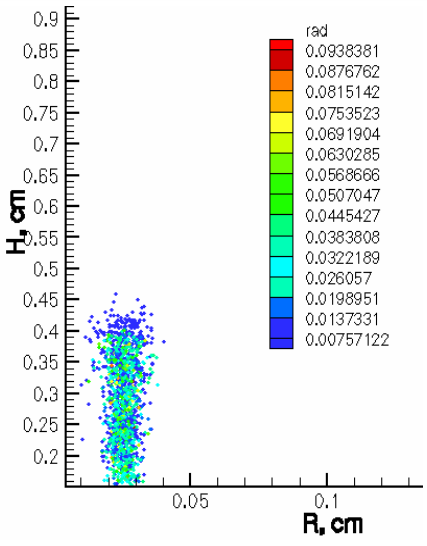

b)

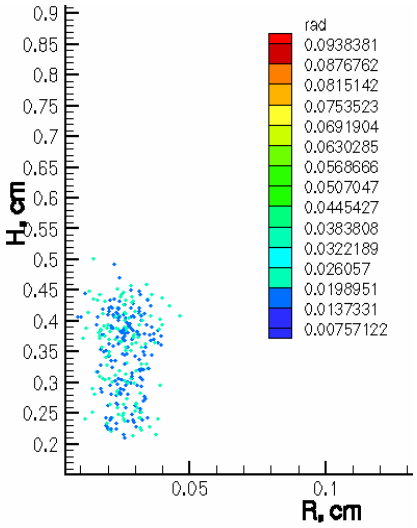

c)

Figure 1. Distribution of octane droplets by size (rad, mm) in the space of the combustion chamber at a pressure of 100 bar at different times
a) $t=10^{-4}$ s, b) $t=3.9\cdot10^{-4}$ s, c) $t=1.1\cdot10^{-3}$ s

Figure 2 shows similar studies for another type of fuel - dodecane. For dodecane at a pressure of 80 bar at the time $t = 10^{-4}$s (Fig. 2a), the maximum height of the spray area is 0.38 cm and a width of 0.06 cm, and the droplet sizes range from 6 to 40 microns. When the spraying process is not yet completed $t=5\cdot10^{-4}$s (Fig. 2b), the droplets rise to a great height, in this case the spray area of dodecane droplets is 1.1 cm in height and 0.15 cm in width of the chamber. A further increase in the injection time leads to a significant decrease in the droplet propagation area (Fig. 2c).

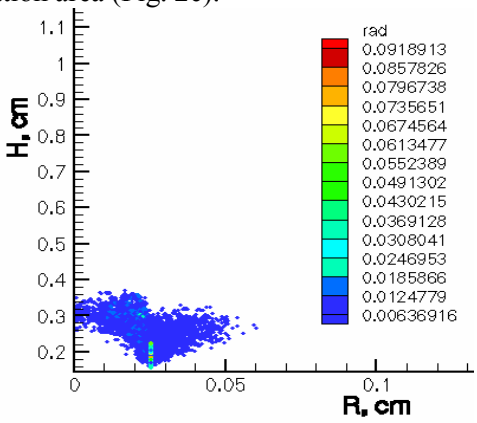

a)

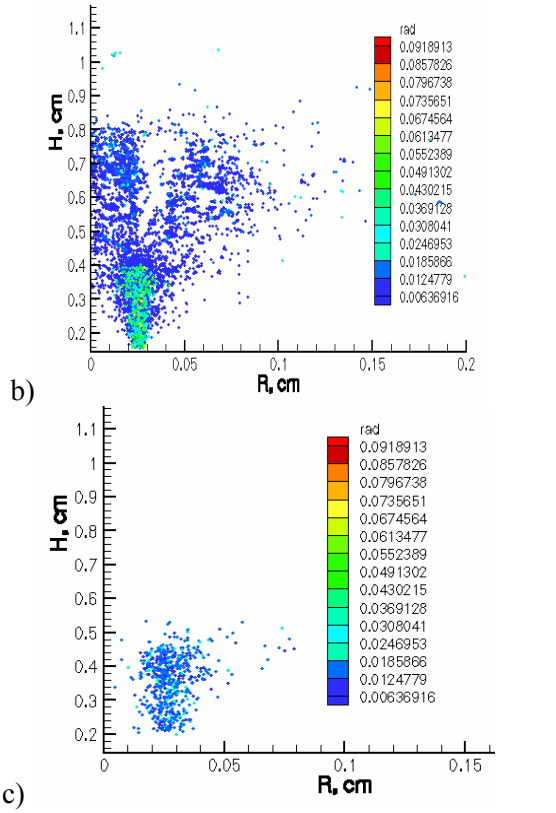

Figure 2. Size distribution of dodecane droplets (rad, mm) in the space of the combustion chamber at a pressure of 80 bar at different times
a) $t=10^{-4}$ c, b) $t=5\cdot10^{-4}$ c, c) $t=1\cdot10^{-3}$ c

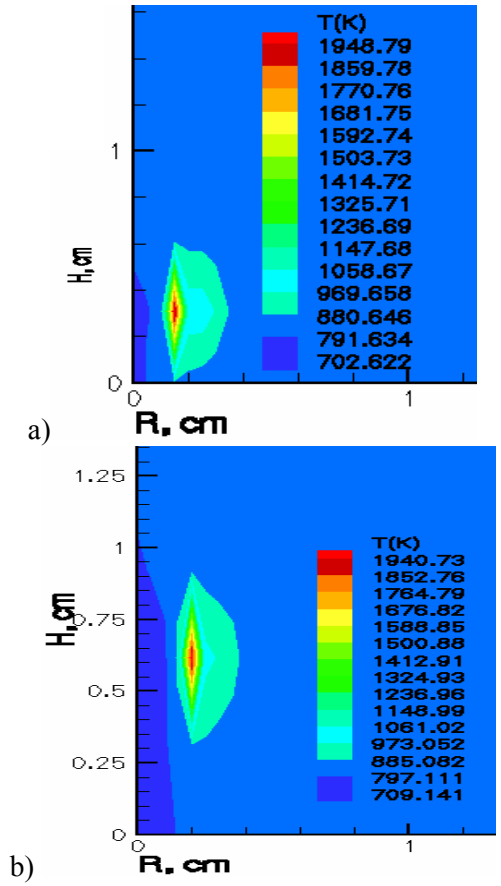

Figure 3. Temperature distribution (T, K) in the space of the combustion chamber at the time of ignition
a) octane P=100 bar and $t=7\cdot10^{-4}$ s, b) dodecane P=80 bar and $t=8.1\cdot10^{-4}$ s

The combustion mechanism of liquid fuels is characterized by the fact that the boiling point of liquid fuels is always lower than the self-ignition temperature, therefore, the combustion of liquid fuels occurs in the vapor phase. The combustion mechanism of liquid fuels includes several stages: a spark (or other foreign source), ignition of the vapor-air mixture, combustion of the vapor-air mixture at the surface of the liquid, an increase in the evaporation rate due to heat transfer from the flame (until equilibrium is reached). The ignition temperature of liquid fuel is the temperature of heating the liquid base of the fuel, at which the fuel droplets ignite and the fuel burns continuously.

As can be seen from Fig. 3, ignition for different fuels occurs at different times. For octane, the ignition moment is $t=7\cdot10^{-4}$ s, while for dodecane $t=8.1\cdot10^{-4}$ s.

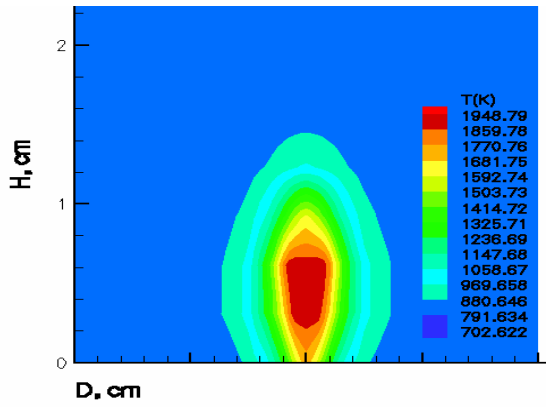

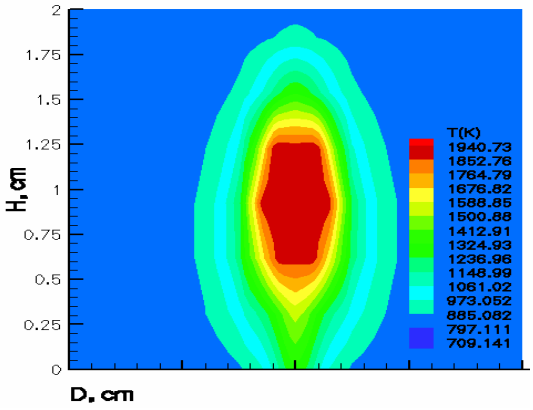

b)

Figure 4. Distribution of the maximum temperature (T, K) in the space of the combustion chamber at the moment of time t=1.5 ·10^{-3} s
a) octane at P=100 bar, b) dodecane at P=80 bar

When liquid fuel is atomized in a stationary or moving gas, a two-phase reacting jet is formed, which burns, forming a torch of liquid fuel. As shown in Fig. 4 (a, b), for both octane and dodecane, at high pressure in the combustion chamber, the high temperature region increases.

The gas temperature distributions in the space of the combustion chamber make it possible to see small differences in the combustion of two types of fuels with the optimal liquid fuel injection mass: the highest temperature is observed when burning octane 1948.79 K (Fig. 4a). When the mixture of fuel vapors with an oxidizer is ignited, the fuel begins to burn very quickly, almost the entire area of the chamber is covered in width by a torch. At the time t=1.5·10^{-3}s, the region of high temperatures for octane (Fig. 4a) is the smallest. Octane vapor rises to a height of 1.5 cm, while dodecane vapor reaches 1.79 cm. For optimal injection masses (for 6 mg octane and 7 mg dodecane), at the final time point (4 ms), the fuel has reacted with the oxidizer completely, without a trace.

A graphical dependence of the size distribution of octane and dodecane droplets (Fig. 5,9), temperature of droplets of both fuels (Fig. 6,10), carbon dioxide concentration (Fig. 7,11) and soot concentration (Fig. 8,12) is plotted depending on the mass of liquid fuel in the combustion chamber.

The dependence of the maximum size of octane droplets on its injection mass is shown in Figure 5. Analysis of the graph shows that an increase in the mass of octane injection to 6 mg leads to a decrease in the size of its droplets and is 93.61 microns. A further increase in mass leads to a slight increase in the radius of fuel droplets. Figure 6 shows the distribution of the maximum temperature of droplets over the volume of the combustion chamber from the injected mass of octane. As we can see, increasing the mass of the injection leads to a slight increase in temperature to 561 K for octane at 6 mg. A further increase in mass leads to a subsequent decrease in temperature. This result agrees with the previous Fig. 5, thus, with a decrease in the radius of the fuel droplets, the temperature of the octane droplets increases due to the intensive evaporation of the fuel.

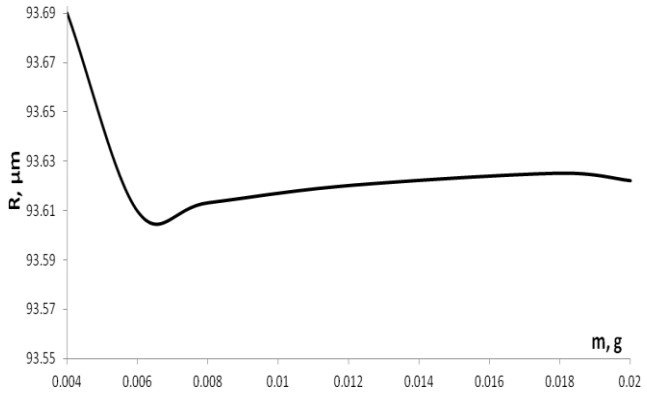

Figure 5. Size distribution of droplets (R, µm) depending on the mass of liquid fuel (m, g) in the combustion chamber

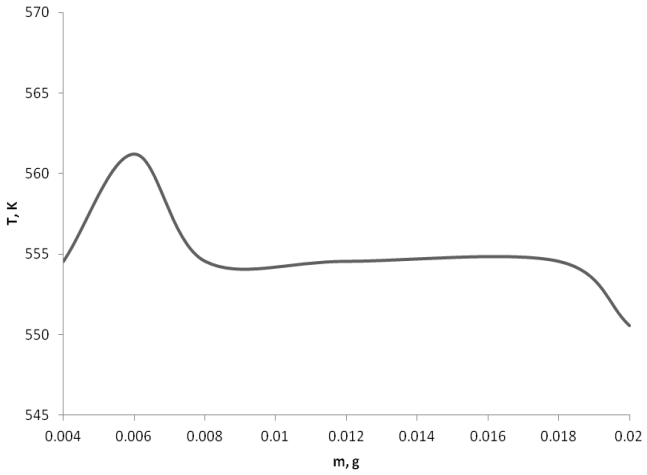

Figure 6. Temperature distribution of drops (T, K) in the combustion chamber depending on the mass of liquid fuel (m, g)

Thus, we can make a preliminary conclusion that the optimal mass of octane can be called equal to 6 mg, at which the droplet sizes are minimal and the droplet temperature reaches its maximum. A further increase in the mass of injection of octane worsens the combustion process.

Figure 7 shows the effect of octane mass on the distribution of carbon dioxide concentration. As the mass of liquid fuel increases, the amount of carbon dioxide increases for obvious reasons: the more fuel, the more CO_2 is formed. The minimum concentration of carbon dioxide equal to 0.0989 g/g

is formed by injecting octane with a mass equal to 6 mg. This result once again confirms that the optimal mass values for two fuels selected above are correct. Figure 8 shows the effect of octane mass on the soot concentration distribution in the combustion chamber space. With an increase in the mass of injected fuel, the soot concentration decreases monotonically, which is consistent with the previous Fig. 7. With an injection mass of 6 mg for octane, a small amount of soot is released equal to 58.4 g/m^3. Thus, the optimal value of the injected mass of octane was obtained equal to 6 mg, at which the size of fuel droplets is minimal 93.61 microns, and the temperature of its drops is maximum 561 K. It is at this value of the mass of octane that a small amount of soot is released 58.4 g/m^3 and the minimum amount carbon dioxide 0.0989 g/g.

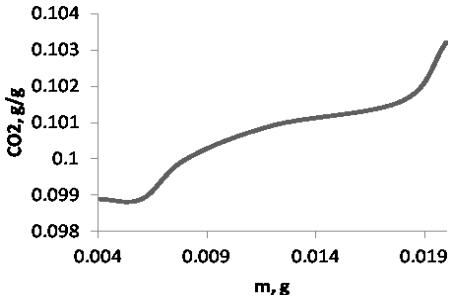

Figure 7. Distribution of carbon dioxide concentration (g/g) in the combustion chamber depending on the mass of liquid fuel (m, g)

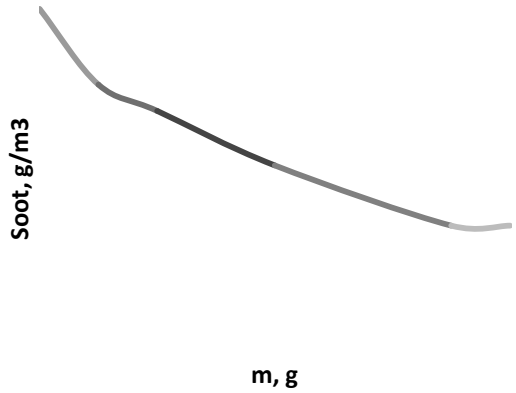

Fihure 8. Distribution of soot concentration (g/m^3) in the combustion chamber depending on the mass of liquid fuel (m, g)

The dependence of the maximum size of dodecane droplets on its injection mass was obtained (Fig. 9), which shows that an increase in the injection mass from 4 mg to 7 mg leads to a decrease in the size of fuel droplets. With a fuel mass of 7 mg, the droplet size reaches its minimum and is 93.754 μm, and the maximum droplet temperature is 644 K (Fig. 10). A further increase in the mass of dodecane leads to a slight increase in the radius of its droplets (Fig. 9) and a subsequent decrease in temperature (Fig. 10).

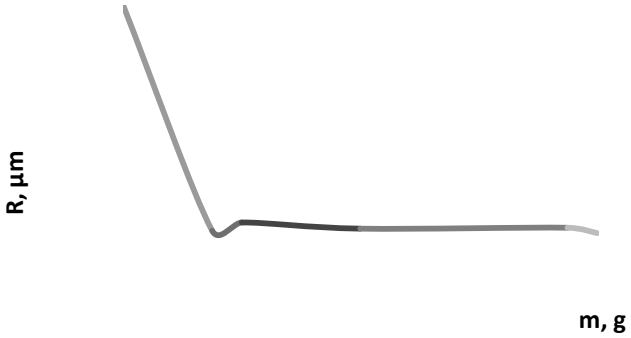

Figure 9. Size distribution of droplets (R, μm) depending on the mass of liquid fuel (m, g) in the combustion chamber

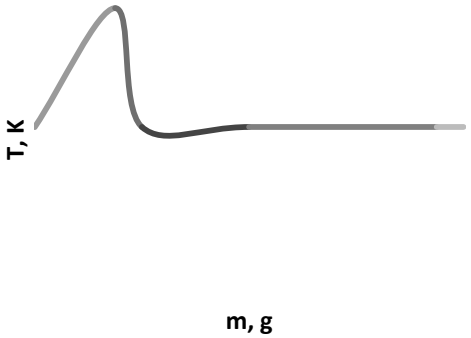

Figure 10. Temperature distribution of drops (T, K) in the combustion chamber depending on the mass of liquid fuel (m, g)

Figure 11 shows the distribution of carbon dioxide concentration depending on the mass of dodecane injected. As can be seen from the figure, for obvious reasons, with an increase in the mass of fuel, the concentration of carbon dioxide increases. With a mass of fuel equal to 7 mg, the minimum amount of CO_2 is formed, which is 0.101 g/g. We can make a preliminary conclusion that the optimal value of the mass of dodecane is 7 mg, at which the concentration of carbon dioxide is minimal and the temperature of the fuel droplets is maximum.
An analysis of the dependence of the mass of liquid fuel on the soot concentration in the space of the combustion chamber (Fig. 12) shows the opposite picture than in the case of CO_2, with an increase in the injection mass, the soot concentration decreases. For dodecane, the minimum amount of soot 25.3 g/m^3 is formed by injecting fuel with a mass of 7 mg.

As a result of the foregoing, the optimal value of the mass of dodecane was obtained equal to 7 mg, at which the size of the fuel droplets is minimal and amounts to 93.754 microns, the maximum temperature of its drops reaches 644 K, at this value of the injection mass a small amount of soot 25.3 g/m^3 and carbon dioxide are released 0.101 g/g.

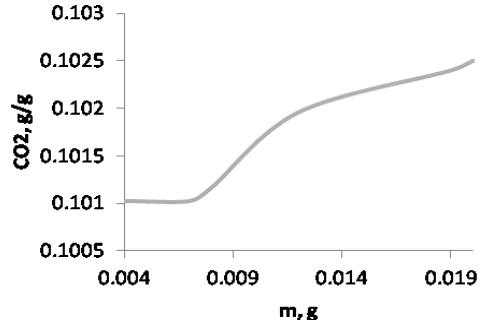

Figure 11. Distribution of carbon dioxide concentration (g/g) in the combustion chamber depending on the mass of liquid fuel (m, g)

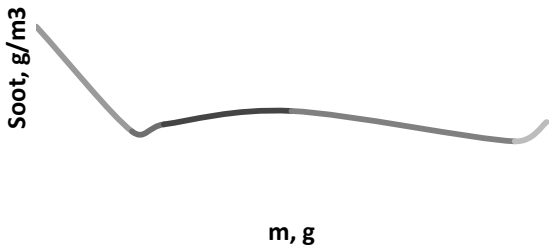

Figure 12. Distribution of soot concentration (g/m^3) in the combustion chamber depending on the mass of liquid fuel (m, g)

For a more profitable organization of the combustion process of liquid fuel (octane and dodecane) in relation to its injected mass under the conditions of this task, it was established:

1) For octane, the optimal mass is 6 mg, because it is at this mass value that the size of its droplets is minimal 93.61 microns, which leads to an increase in the spray area and intensive evaporation of the fuel. The evaporation temperature of octane droplets is maximum 561 K, which increases the efficiency of fuel combustion. To minimize emissions of harmful substances, the optimal mass of octane was chosen equal to 6 mg, at which a small amount of soot 58.4 g/m^3 and a minimum amount of carbon dioxide 0.0989 g/g are released.

2) The optimal value of the mass of dodecane is 7 mg, in this case the spray area of dodecane droplets is maximum, and the size of fuel droplets is minimum and is 93.754 microns. Dodecane drops are heated to a maximum temperature of 644 K. At this dodecane injection mass, the following reaction products are formed: soot, the concentration of which is 25.3 g/m^3 and a small amount of carbon dioxide 0.101 g/g.

4 Conclusion

The paper describes the main features of the combustion of liquid fuel injections, developed a stochastic model for the atomization of liquid fuels injected into the combustion chamber at high pressures and high Reynolds numbers.

A stochastic model of atomization of liquid fuels injected into a combustion chamber at high pressures and high Reynolds numbers has been developed. On the basis of the proposed model, computational experiments were carried out to study the combustion of liquid fuel depending on the injected mass in the combustion chamber under given initial conditions in full. A graphical dependence of all these characteristics has been constructed, namely, the distribution of octane droplets by size, the temperature of octane droplets, carbon dioxide concentration and soot concentration depending on the mass of liquid fuel in the combustion chamber.

When studying the effect of the mass of liquid fuel on the processes of ignition and combustion at high pressures and high Reynolds numbers, the mass values for octane 6 mg and for dodecane 7 mg were taken as the most optimal. With an octane mass of 6 mg, the droplet sizes are minimal and equal to 93.61 μm, and the temperature reaches its maximum of 561 K. In this case, a small amount of CO_2 is released, equal to 98.89 and soot, 58.38 g/m^3. For the same reasons, the optimal weight for dodecane was 7 mg. The maximum droplet size is 93.75 μm, the temperature of dodecane droplets is 644.6 K. In this case, CO_2 is formed equal to 10.1 and soot – 25.51 g/m^3. A further increase in the injection mass, both for octane and dodecane at optimal pressures, worsens the combustion process. The results obtained are of fundamental and practical importance and can be used to develop the theory of combustion of gaseous and liquid fuels.

References:

[1] Vinkovic I., Simoens S., Gorokhovski M. Large eddy simulation of droplet dispersion for inhomogeneous turbulent wall flow, *Int. J. of Multiphase Flow*, Vol. 32, № 3, 2005, pp. 344-364.

[2] Bolegenova S.A., Maximov V.Yu., et al. Simulation of nitrogen oxides formation as air pollution on the example of real combustion furnace, *WSEAS Trans on Fl Mech,* Vol. 16, 2021, pp. 192- 200.
[3] Heierle E.I., Manatbayev R., et al. CFD study of harmful substances production in coal-fired power plant of Kazakhstan, *Bulgarian Chemical Communications*, Vol. 48, 2016, pp. 260-265.
[4] Bekmukhamet A., Gabitova Z. et al. Control of harmful emissions concentration into the atmosphere of megacities of Kazakhstan Republic, *International Conference on Future Information Engineering (FIE 2014)*, 2014, pp. 252–258.
[5] Muller H. *Numerische simulation von Feuerungen. CFD,* Braunschweig: IWBT, 1997.
[6] Pilipenko N.V., Baktybekov K.S., Syzdykov A.B. et al. Investigation of the different Reynolds numbers influence on the atomization and combustion processes of liquid fuel, *Bulgarian Chemical Communications*, Vol. 50, Special Issue G, 2018, pp. 68-77.
[7] Horst M., Askarova A., Yevgeniya H., Reinhard L. CFD code FLOREAN for industrial boilers simulations, *WSEAS Transactions on Heat and Mass Transfer*, Vol. 4, No. 4, 2009, pp. 98-107.
[8] Maximov V.Yu., Beketayeva M.T. et al 3D visualization of the results of using modern OFA technology on the example of real boiler, *WSEAS TRANSACTIONS on FLUID MECHANICS*, Vol. 16, 2021, pp. 232-238.
[9] Oran E., Boris J. *Numerical simulation of reactive flows*, Mir, 1990.
[10] Amsden A.A., O'Rourke P.J., Butler T.D. *KIVA-II: A computer program for chemically reactive flows with sprays*, Los Alamos, 1989.
[11] Zaitsev S.A., Kuznetsov V.R., Kuntsev G.M. *Influence of heating and evaporation of liquid fuel on combustion in a model combustion chamber*, Physics of Combustion and Explosion, 1991.
[12] O'Rourke P.J. *Collective Drop Effects on Vaporizing Liquid Sprays*, Ph.D thesis, Princeton University, Princeton, NJ, 1981.
[13] O'Rourke P.J., Amsden A.A. The TAB Method for Numerical Calculations of Spray Droplet Breakup, *SAE Tech. Paper 872089*, 1987.
[14] Reitz R.D. Modeling Atomization Processes in High – Pressure Vaporizing Sprays, *Atomization and Sprays Technol*., Vol. 3, 1987, pp. 309-337.
[15] Ibrahim E.A., Yang H.Q., Pizekwas A.J. Modeling of Spray Droplets Deformation and Breakup, *AIAA J. Propulsion*, Vol. 9, № 4, 1993, pp. 651-654.
[16] Gorokhovsky M.A., Loktionova I.V., et al. Combustion of liquid fuels in a combustion chamber, *Proceedings of the National Academy of Sciences of the Republic of Kazakhstan, a series of physical and mathematical*, Vol. 3, 2006, pp. 10-14.

Contribution of individual authors to the creation of a scientific article (ghostwriting policy)

Aliya Askarova, Saltanat Bolegenova has organized and executed the experiments.
Valeriy Maximov and Meruyert Beketayeva carried out the simulation results, interpretation (discussion) and verification of results.

Follow: www.wseas.org/multimedia/contributor-role-instruction.pdf

Sources of funding for research presented in a scientific article or scientific article itself

Research funded by the Ministry of Education and Science of the Republic of Kazakhstan

Creative Commons Attribution License 4.0 (Attribution 4.0 International , CC BY 4.0)